

## Supporting Information for:

# An “Anion-Switchable” Pincer-Mn(I) Catalyst for the Reductive N-Methylation of Amines with Formic Acid and CO<sub>2</sub>

*Sebastián Martínez-Vivas, Sergio Gonell, Macarena Poyatos and Eduardo Peris*

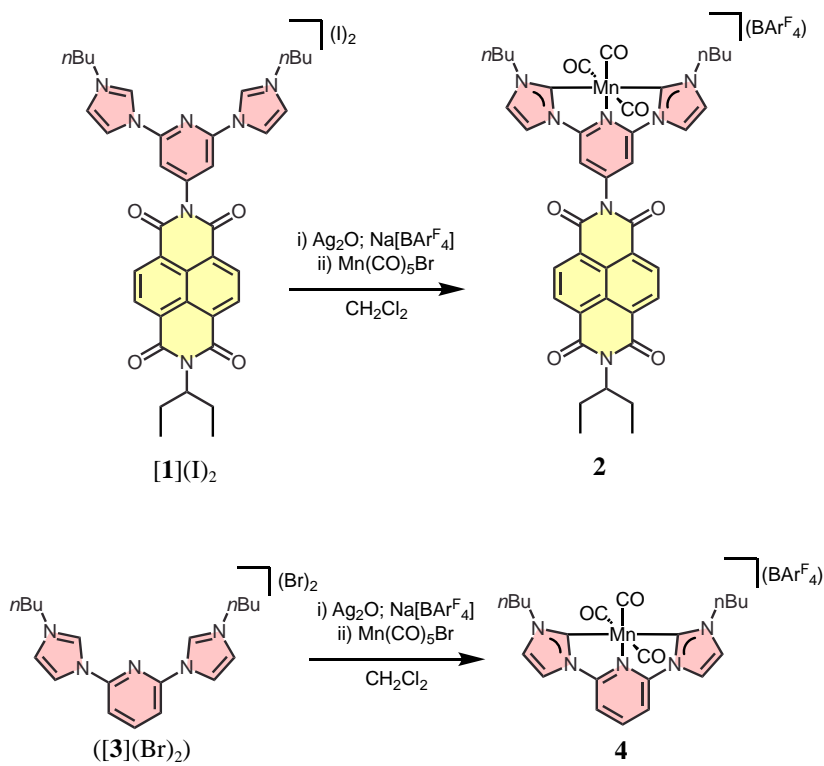
<sup>a</sup>Institute of Advanced Materials (INAM). Centro de Innovación en Química Avanzada (ORFEO-CINQA). Universitat Jaume I. Av. Vicente Sos Baynat s/n. Castellón. E-12006. Spain. Email: poyatosd@uji.es; eperis@uji.es.

<b>General considerations</b>	<b>S1</b>
<b>1. Synthesis and characterization of the compounds</b>	<b>S2-S4</b>
<b>2. Spectroscopic data</b>	<b>S5-S7</b>
2.1. <sup>1</sup> H and <sup>13</sup> C{ <sup>1</sup> H NMR spectra of <b>2</b>	S5
2.2. <sup>1</sup> H and <sup>13</sup> C{ <sup>1</sup> H} NMR spectra of <b>4</b>	S6
2.3. IR spectroscopy of complexes <b>2</b> and <b>4</b>	S7
<b>3. Electrochemical studies</b>	<b>S8-S12</b>
3.1. Electrochemical measurements	S8
3.2. Spectroelectrochemical studies	S10
<b>4. Study of the Cl<sup>-</sup>/NDI interaction</b>	<b>S13-S15</b>
4.1 Study of the Cl <sup>-</sup> /NDI interaction by IR	S13
4.2. Study of the Cl <sup>-</sup> /NDI interaction by UV-Vis	S14
4.3. Study of the Cl <sup>-</sup> /NDI interaction by <sup>1</sup> H NMR	S15
<b>5. Catalytic studies</b>	<b>S16-S21</b>
5.1. Methylation of <i>N</i> -ethylaniline using formic acid	S16
5.2. Redox switching experiments	S18
5.3. Determination of the reaction order with respect to the catalyst	S20
5.4. Study of the scope of the reaction	S21
5.5. Methylation of <i>N</i> -ethylaniline using CO <sub>2</sub>	S22
<b>6. References</b>	<b>S23</b>

**General considerations**

Bis-imidazolium salt **[1]**(I)<sub>2</sub><sup>1</sup> and 2,6-bis(1-*n*-butylimidazolium-3-yl)pyridine bromide (**[3]**(Br)<sub>2</sub>)<sup>2</sup> were prepared as described in the literature. The solvents were dried using a solvent purification system (SPS M BRAUN) or purchased and degassed prior to use by purging them with dry nitrogen. All the other reagents were used as received from the commercial suppliers. Column chromatography was performed using silica gel (60-120 mesh). NMR spectra recorded on a Bruker 300 MHz using CD<sub>2</sub>Cl<sub>2</sub> or CD<sub>3</sub>CN as solvents, chemical shifts ( $\delta$ ) are expressed in ppm using the residual proton resonance of the solvent as an internal standard. To verify the bulk purity of the Mn(I) complexes **2** and **4**, their <sup>1</sup>H NMR spectra were carried out in the presence of an equimolar amount of 1,3,5-trimethoxybenzene. All coupling constants (*J*) are expressed in hertz (Hz). Electrospray mass spectra (ESI-MS) were recorded on a Micromass Quatro LC instrument; nitrogen was employed as drying and nebulizing gas. Infrared spectra (FTIR) were performed on a Bruker Equinox 55 spectrometer with a spectral window of 4000-400 cm<sup>-1</sup>. UV-Visible absorption spectra were recorded on a Varian Cary 300 BIO spectrophotometer under ambient conditions.

## 1. Synthesis and characterization of the compounds

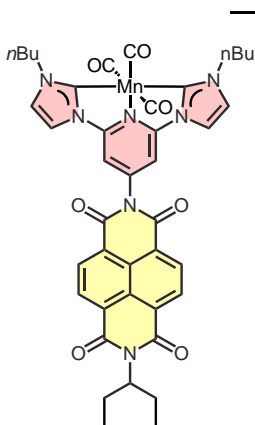


**Scheme S1.** Synthesis of the NHC-based pincer complexes described in this work

### 1.1. General procedure for the coordination to Mn(I)

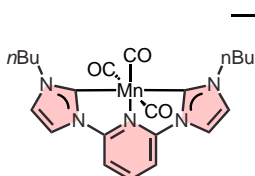
The corresponding bis-imidazolium salt (1 equiv.),  $\text{Na}(\text{BArF}_4)$  (1.10 equiv.) and  $\text{Ag}_2\text{O}$  (1 equiv.) were placed together in a Schlenk tube fitted with a Teflon cap. The tube was evacuated and filled with nitrogen three times. The solids were suspended in  $\text{CH}_2\text{Cl}_2$  (4 mL) and stirred at room temperature in the absence of light overnight. After this time, the suspension was filtered through Celite into a Schlenk tube charged with  $[\text{Mn}(\text{CO})_5\text{Br}]$  (1 equiv.). The suspension was stirred in the absence of light for 48h at 60 °C. Afterward, it was passed through a column chromatography using dichloromethane as eluent.

**Synthesis and characterization of 2.** Complex **2** was prepared employing the general procedure by reacting **[1](I)<sub>2</sub>** (200 mg, 0.219 mmol),  $[\text{Mn}(\text{CO})_5\text{Br}]$  (60.2 mg, 0.219 mmol),  $\text{Na}[\text{BArF}_4]$  (213.5 mg, 0.241 mmol) and  $\text{Ag}_2\text{O}$  (50.7 mg, 0.219 mmol). Complex **2** was



isolated as a yellow solid in 30% yield (109 mg). Elemental analysis calcd (%) for  $C_{73}H_{51}N_7O_7MnBF_{24}$ : C, 52.82; H, 3.10; N, 5.91. Found C, 52.69; H, 3.29; N, 5.74.  $^1H$  NMR (300 MHz,  $CD_2Cl_2$ ):  $\delta$  8.83 (s, 4H,  $CH_{NDI}$ ), 7.75 (d,  $^3J_{H-H} = 1.8$  Hz, 2H,  $CH_{imid}$ ), 7.73-7.68 (m, 8H,  $Ar^F$ ), 7.54 (br s, 4H,  $Ar^F$ ), 7.48 (s, 2H,  $CH_{pyr}$ ), 7.31 (d,  $^3J_{H-H} = 1.9$  Hz, 2H,  $CH_{imid}$ ), 5.09-4.98 (m, 1H,  $CH(CH_2CH_3)_2$ ), 4.31 (t,  $^3J_{H-H} = 7.4$  Hz, 4H,  $CH_2CH_2CH_2CH_3$ ), 2.31-2.14 (m, 2H,  $CH(CH_2CH_3)_2$ ), 2.05-1.90 (m, 6H; 2H,  $CH(CH_2CH_3)_2$  and 4H,  $CH_2CH_2CH_2CH_3$ ), 1.58-1.46 (sext,  $^3J_{H-H} = 7.7$  Hz, 4H,  $CH_2CH_2CH_2CH_3$ ), 1.04 (t,  $^3J_{H-H} = 7.3$  Hz, 6H,  $CH_2CH_2CH_2CH_3$ ), 0.93 (t,  $^3J_{H-H} = 7.5$  Hz, 6H,  $CH(CH_2CH_3)_2$ ).  $^{13}C$   $\{^1H\}$  NMR (75 MHz,  $CD_2Cl_2$ ):  $\delta$  208.2 (Mn-CO), 206.2 (Mn-CO), 204.1 (Mn- $C_{carbene}$ ), 163.0 ( $C_{NDI=O}$ ), 162.6 (q,  $^1J_{CB} = 49.5$  Hz,  $Ar^F$ ), 153.4 ( $C_{pyr-imid}$ ), 149.8 ( $C_{pyr-NDI}$ ), 135.4 ( $Ar^F$ ), 132.6 ( $CH_{NDI}$ ), 129.6 (m,  $Ar^F$ ), 129.2 (m,  $Ar^F$ ), 127.6 ( $Ar^F$ ), 126.8 ( $CH_{imid}$ ), 123.3 ( $Ar^F$ ), 118.0 (m,  $Ar^F$ ), 118.0 ( $CH_{imid}$ ), 107.9 ( $CH_{pyr}$ ), 59.1 ( $CH(CH_2CH_3)_2$ ), 52.4 ( $CH_2CH_2CH_2CH_3$ ), 33.4 ( $CH_2CH_2CH_2CH_3$ ), 25.5 ( $CH(CH_2CH_3)_2$ ), 20.4 ( $CH_2CH_2CH_2CH_3$ ), 13.9 ( $CH_2CH_2CH_2CH_3$ ), 11.6 ( $CH(CH_2CH_3)_2$ ). HRMS (20 V, m/z): 796.2296  $[M]^+$ . (Calcd. for  $[M]^+$ : 796.2291). IR ( $CH_3CN$ ):  $\nu(CO)$  2051, 1968 and 1914  $cm^{-1}$ .

**Synthesis and characterization of 4.** Complex 4 was prepared employing the general



procedure by reacting [3](Br)<sub>2</sub> (200 mg, 0.412 mmol),  $[Mn(CO)_5Br]$  (111.0 mg, 0.412 mmol),  $Na(BAr^F_4)$  (401.6 mg, 0.453 mmol) and  $Ag_2O$  (95.5 mg, 0.412 mmol). Complex 4 was isolated as yellow oil in 45% yield (239 mg). The hygroscopic

nature of complex 4 prevented its satisfactory elemental analysis.  $^1H$  NMR (300 MHz,  $CD_2Cl_2$ ):  $\delta$  8.09 (t,  $^3J_{H-H} = 8.2$  Hz, 2H,  $CH_{pyr}$ ), 7.79-7.65 (m, 10H; 2H,  $CH_{imid}$  and 8H,  $Ar^F$ ), 7.55 (br s, 4H,  $Ar^F$ ), 7.32 (d,  $^3J_{H-H} = 8.1$  Hz, 2H,  $CH_{pyr}$ ), 7.26 (d,  $^3J_{H-H} = 1.4$  Hz, 2H,  $CH_{imid}$ ), 4.27 (t,  $^3J_{H-H} = 7.4$  Hz, 4H,  $CH_2CH_2CH_2CH_3$ ), 1.94 (q,  $^3J_{H-H} = 7.5$  Hz, 4H,  $CH_2CH_2CH_2CH_3$ ), 1.53-1.43 (sext,  $^3J_{H-H} = 7.6$  Hz, 4H,  $CH_2CH_2CH_2CH_3$ ), 1.02 (t,  $^3J_{H-H} = 7.3$  Hz, 6H,  $CH_2CH_2CH_2CH_3$ ).  $^{13}C$   $\{^1H\}$  NMR (75 MHz,  $CD_2Cl_2$ ):  $\delta$  208.1 (Mn-CO), 203.4 (Mn- $C_{carbene}$ ), 197.5 (Mn-CO), 162.4 (q,  $^1J_{CB} = 49.5$  Hz,  $Ar^F$ ), 152.7 ( $C_{pyr-imid}$ ), 143.7 ( $CH_{pyr}$ ), 135.4 ( $Ar^F$ ), 129.6 (m,  $Ar^F$ ), 129.2 (m,  $Ar^F$ ), 127.0 ( $Ar^F$ ), 126.6 ( $CH_{imid}$ ), 123.4 ( $Ar^F$ ), 118.0 (m,  $Ar^F$ ), 117.8 ( $CH_{imid}$ ), 106.5 ( $CH_{pyr}$ ), 52.3 ( $CH_2CH_2CH_2CH_3$ ), 33.4 ( $CH_2CH_2CH_2CH_3$ ), 20.3

(CH<sub>2</sub>CH<sub>2</sub>CH<sub>2</sub>CH<sub>3</sub>), 13.9 (CH<sub>2</sub>CH<sub>2</sub>CH<sub>2</sub>CH<sub>3</sub>). HRMS (20 V, m/z): 462.1339 [M]<sup>+</sup>. (Calcd. for [M]<sup>+</sup>: 462.1338). IR (CH<sub>3</sub>CN): ν(CO) 2049, 1965 and 1912 cm<sup>-1</sup>.

## 2. Spectroscopic data

### 2.1. $^1\text{H}$ and $^{13}\text{C}\{^1\text{H}\}$ NMR spectra of **2**

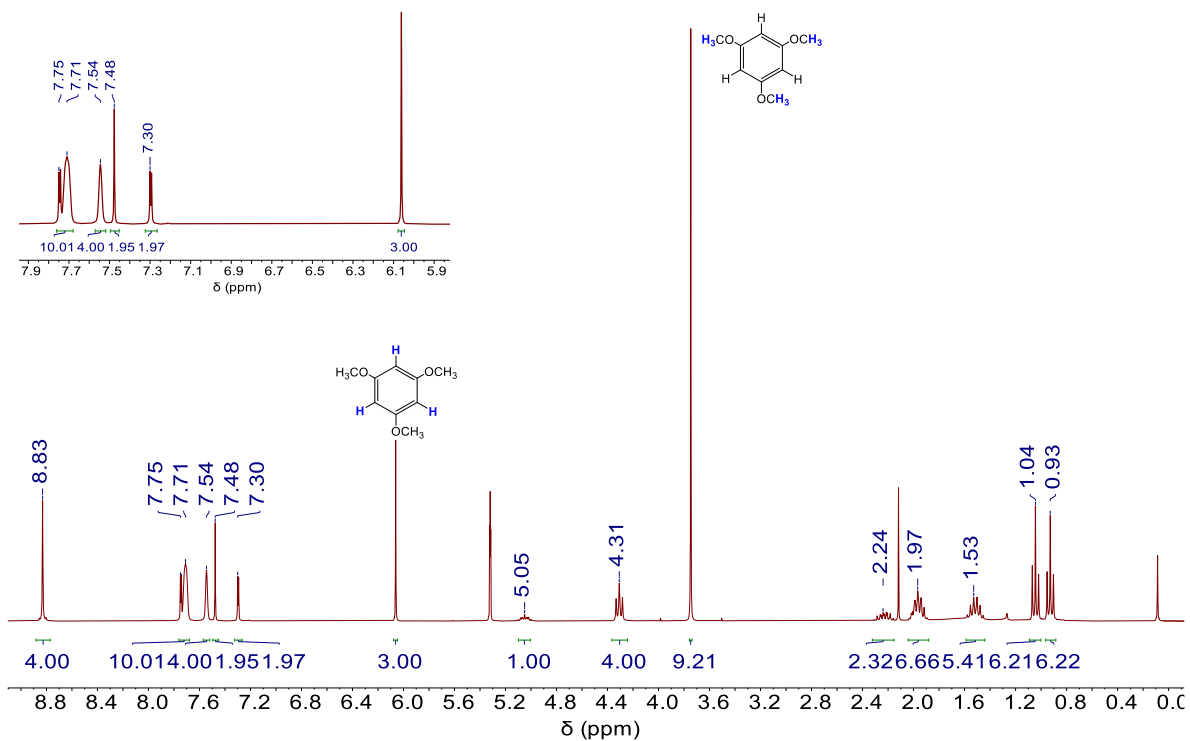


**Figure S1.**  $^1\text{H}$  NMR spectrum (300 MHz,  $\text{CD}_2\text{Cl}_2$ ) of **2** in the presence of an equimolar amount of 1,3,5-trimethoxybenzene

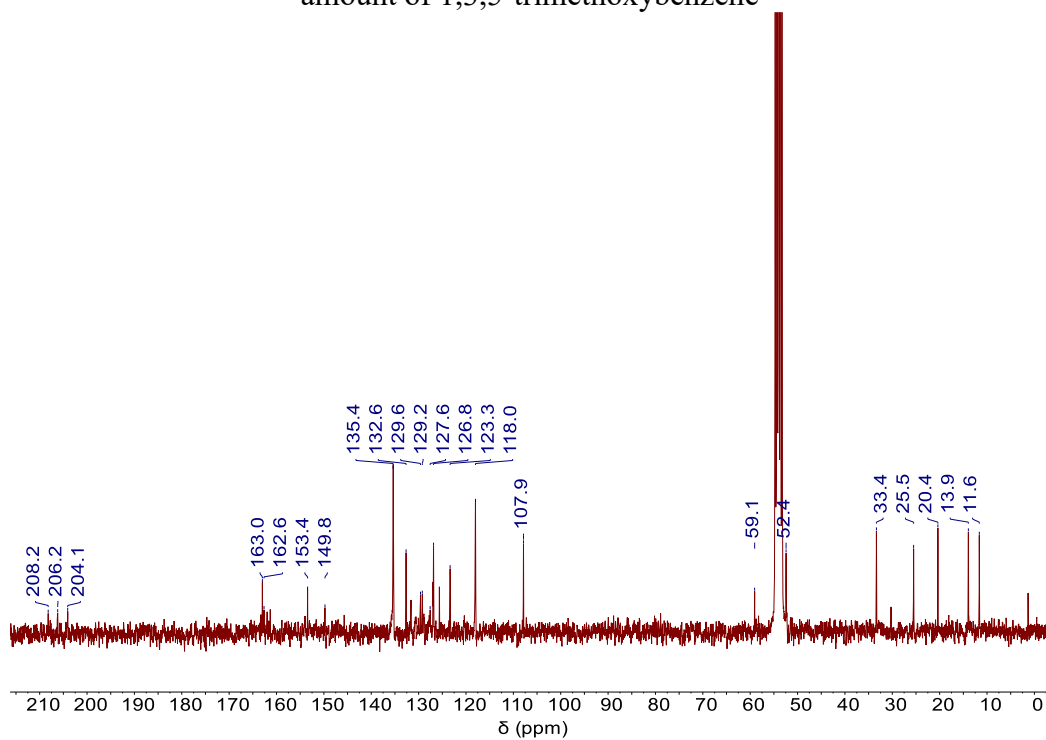


**Figure S2.**  $^{13}\text{C}\{^1\text{H}\}$  spectrum (75 MHz,  $\text{CD}_2\text{Cl}_2$ ) of **2**

## 2.2. $^1\text{H}$ and $^{13}\text{C}\{^1\text{H}\}$ NMR spectra of **4**

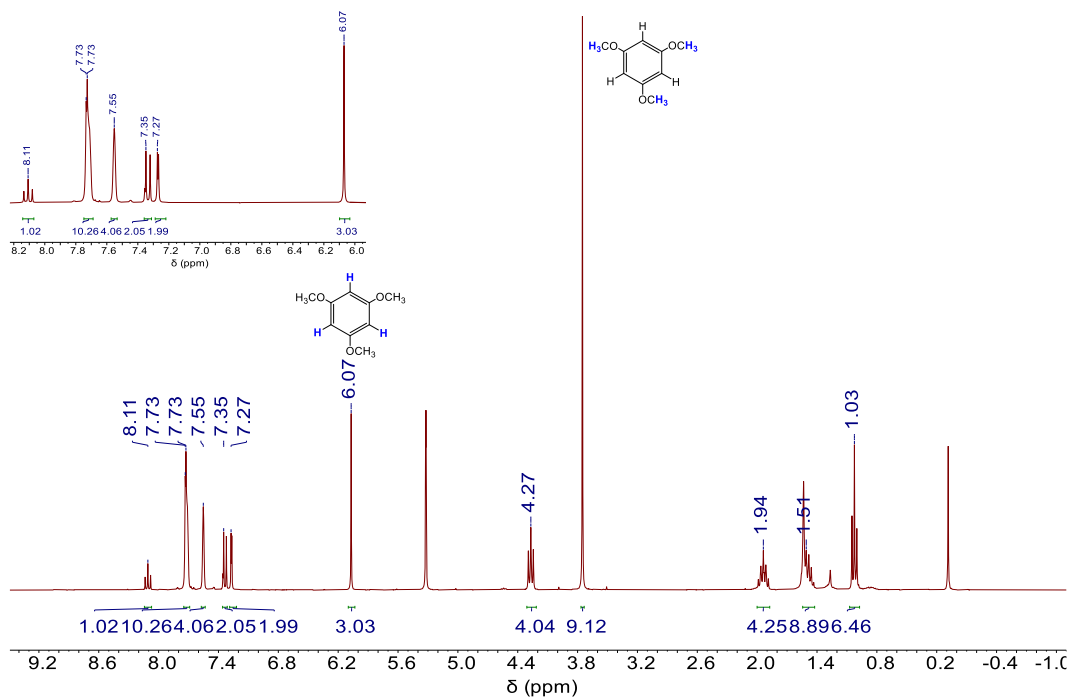


**Figure S3.**  $^1\text{H}$  NMR spectrum (300 MHz,  $\text{CD}_2\text{Cl}_2$ ) of **4** in the presence of an equimolar amount of 1,3,5-trimethoxybenzene

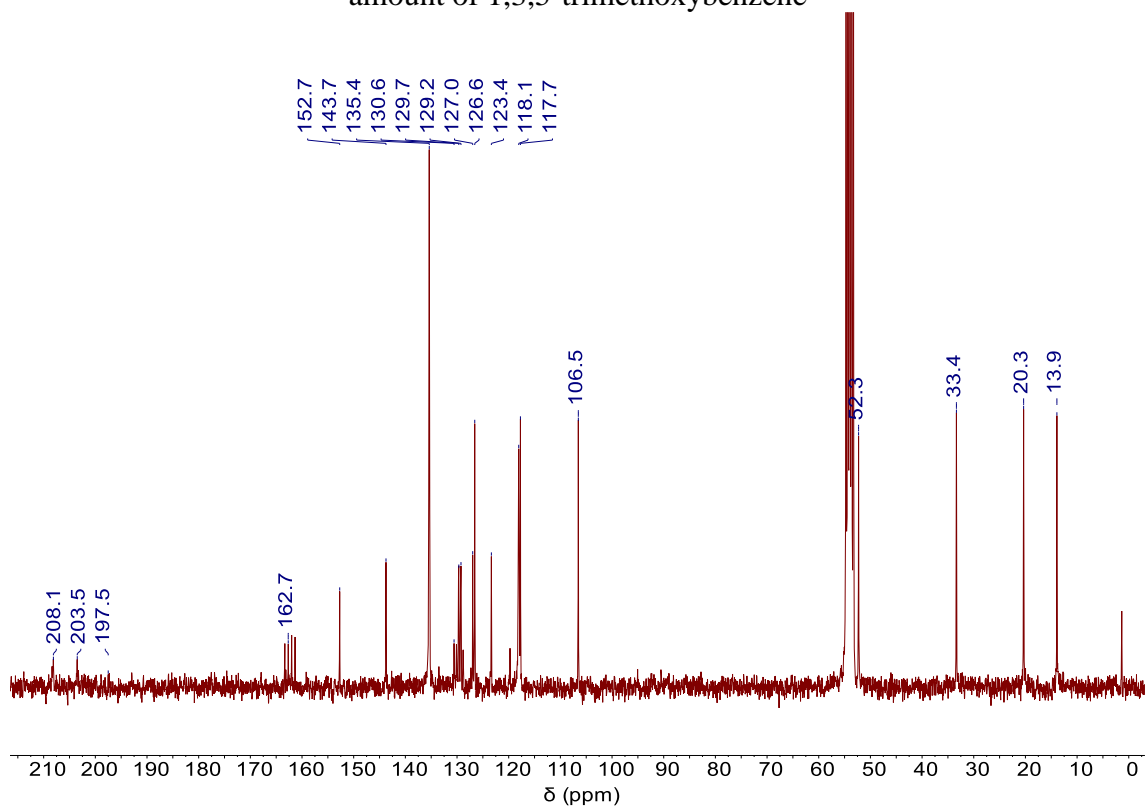


**Figure S4.**  $^{13}\text{C}\{^1\text{H}\}$  spectrum (75 MHz,  $\text{CD}_2\text{Cl}_2$ ) of **4**

### 2.3. IR spectroscopy of complexes **2** and **4**

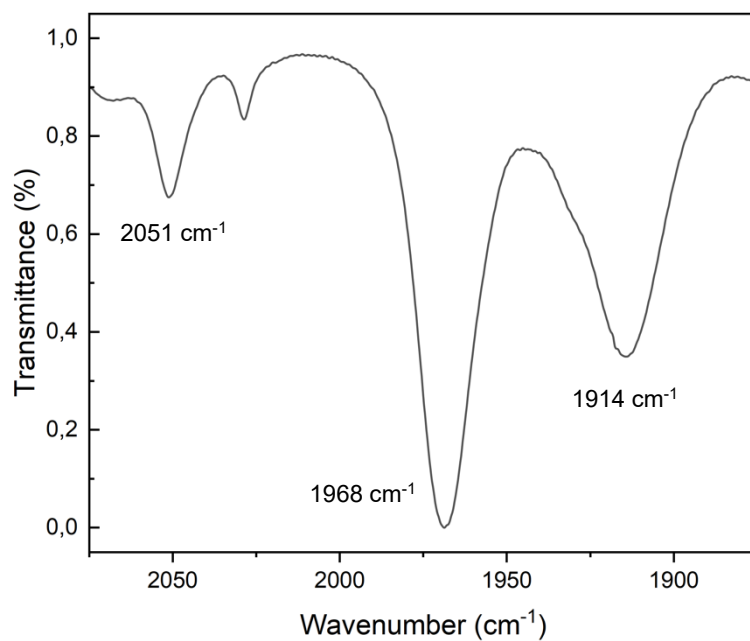


**Figure S5.** IR spectrum of **2** in  $\text{CH}_3\text{CN}$

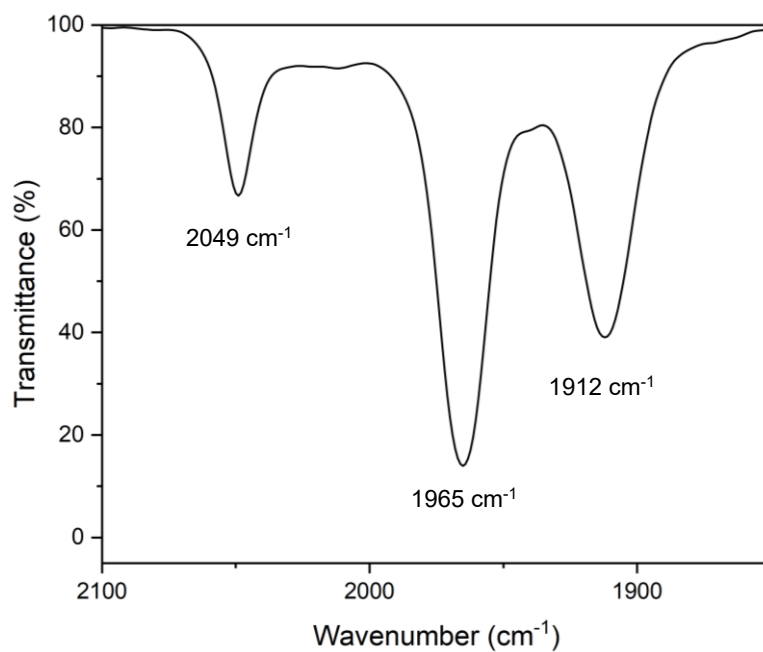


**Figure S6.** IR spectrum of **4** in  $\text{CH}_3\text{CN}$



### 3. Electrochemical studies

#### 3.1. Electrochemical measurements

Electrochemical studies were carried out by using an Autolab Potentiostat, Model PGSTAT101 controlled with NOVA 2.1.5 software. In all experiments,  $[N(nBu)_4][PF_6]$  (0.1 M in dry and deoxygenated acetonitrile) was used as the supporting electrolyte with an analyte concentration of 1 mM. Cyclic voltammetry was performed in a cell, under Ar or CO atmosphere and with a disk glassy carbon working electrode, a platinum counter electrode, and a silver wire pseudoreference electrode. Unless otherwise stated, measurements were performed at  $100\text{ mVs}^{-1}$  scan rate. All scans were referenced to the ferrocenium/ferrocene ( $Fc^+/Fc$ ) couple at 0 V. Ohmic drop was minimized by minimizing the distance between the working and reference electrodes. The residual ohmic drop was estimated by positive feedback and compensated at 95 %.

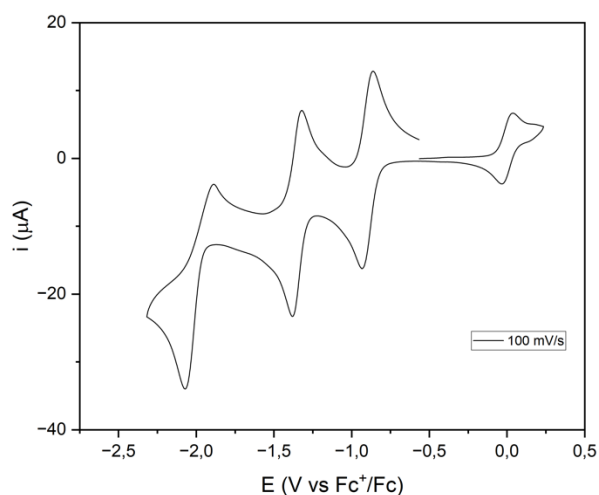


**Figure S7.** Cyclic voltammogram of **2** at 100 mV/s

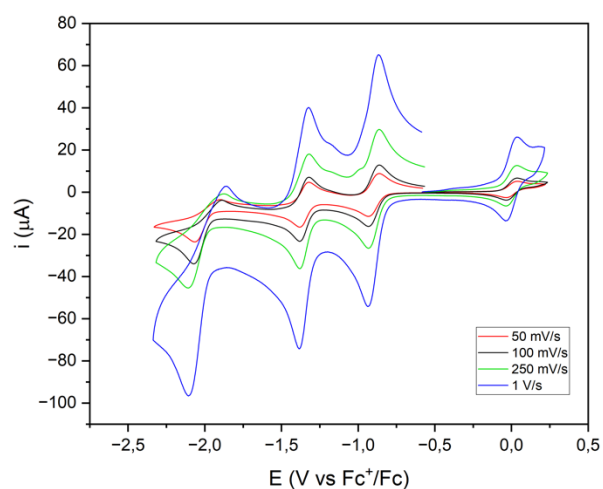


**Figure S8.** Cyclic voltammogram of **2** at different scan rates

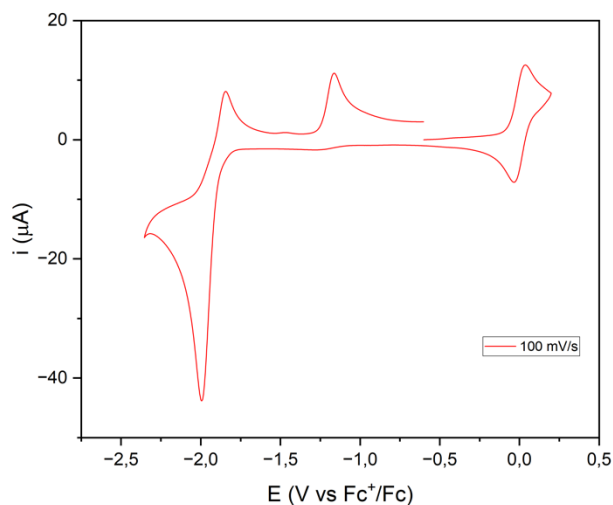


**Figure S9.** Cyclic voltammogram of **4** at 100 mV/s

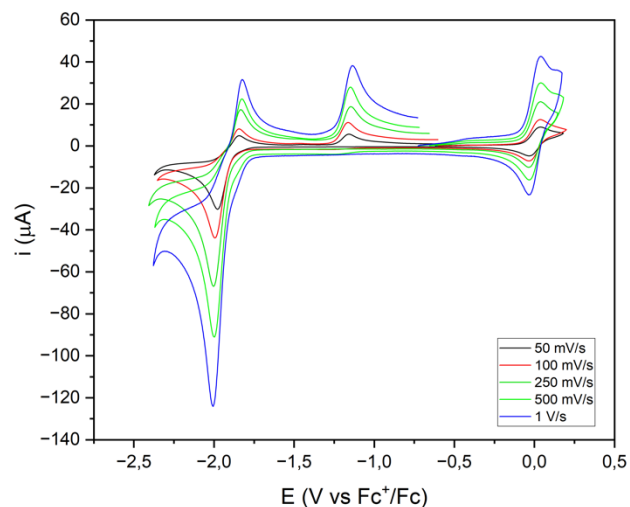


**Figure S10.** Cyclic voltammogram of **4** at different scan rates

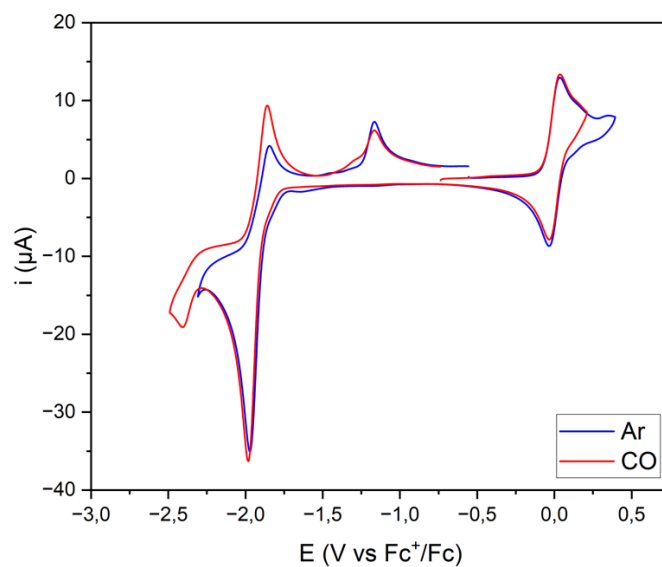
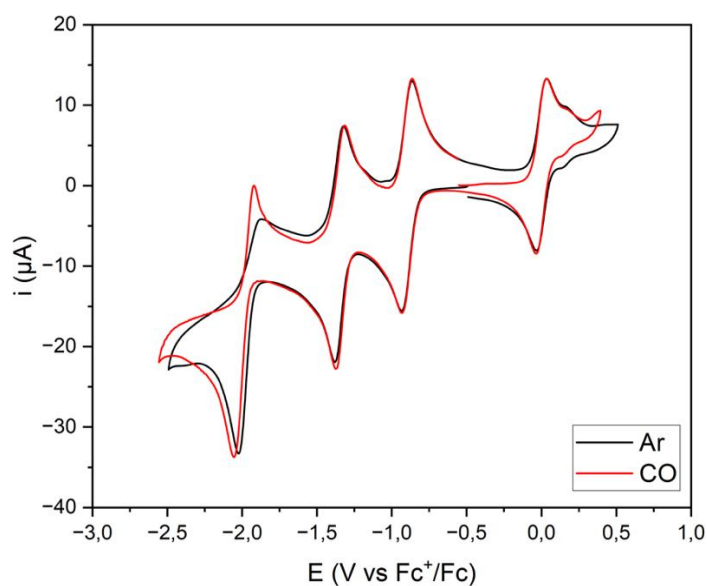


**Figure S11.** Cyclic voltammogram of **2** (right) and **4** (left) performed under Ar and CO saturated atmosphere at 100 mV/s

**Table S1.** Summary of the electrochemical properties of complexes **2** and **4**

Complex	$E_{pc}$ (V)	$E_{pa}$ (V)	$E_{1/2}$ (V)/ $\Delta E$ (mV)	$E_{1/2}$ (V)/ $\Delta E$ (mV)
<b>2</b>	-2.072	-1.889	-1.351/62	-0.898/71
<b>4</b>	-1.994	-1.844	-	-

### 3.2. Spectroelectrochemical studies

Spectroelectrochemical (SEC) measurements were performed using a gastight, optically transparent thin-layer solution cell fabricated by Prof. Hartl at the University of Reading (Reading, U.K.), as described previously.<sup>[7]</sup> The SEC cell contained a masked Pt-minigrad working electrode (32 wires/cm), a Pt-gauze auxiliary electrode and an Ag-wire pseudo-reference electrode and had CaF<sub>2</sub> windows. In each experiment, electrochemical reduction of the species of interest ([Analyte] = 5 mM for IR experiments and 1 mM for UV-vis experiments, [TBAPF<sub>6</sub>] = 100 mM in CH<sub>3</sub>CN under inert atmosphere) was monitored by the appropriate spectroscopy for a period of 2–5 min. First, the potential of the cell was swept negatively starting at the open circuit potential, recording a thin-layer cyclic voltammogram (5 mV/s) to identify the potential window of interest. Then, fresh analyte solution was introduced in the cell and the potential was varied within range of interest in 33 mV steps. The electrolysis step did not exceed 30 s. After each step, an IR or an UV-vis spectrum was collected. Diffusion and mixing of the redox products generated at the working and auxiliary electrodes in the cell were reasonably suppressed within the total experimental time (no more than 5 min for one complete measurement).

As can be seen in the following figures, the stepwise reduction of **2** produced changes in the CO frequencies (Figure S12, Table S2) while no changes were observed upon the reduction of **4** (Figure S13).

**Table S2.** CO stretching frequencies before and after reduction of complex **2**

Species	$\nu_1(\text{CO}) \text{ cm}^{-1}$	$\nu_2(\text{CO}) \text{ cm}^{-1}$	$\nu_3(\text{CO}) \text{ cm}^{-1}$
<b>2</b>	2051	1968	1914
one-electron reduction	2048	1965	1911
two-electron reduction	2048	1962	1908

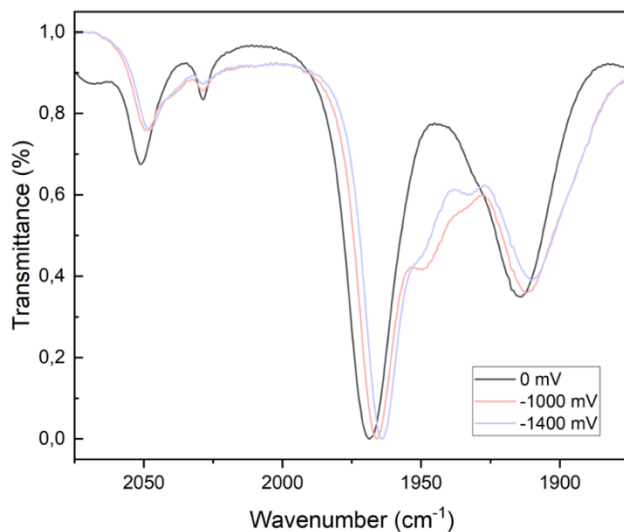


**Figure S12.** IR-SEC reduction of **2** in dry  $\text{CH}_3\text{CN}$  (0.1 M  $[\text{N}(\text{nBu})_4][\text{PF}_6]$ ). The solid lines represent the IR spectra of complex **2** (black) and those of the one-electron reduced (red) and the two-electron reduced species (blue).

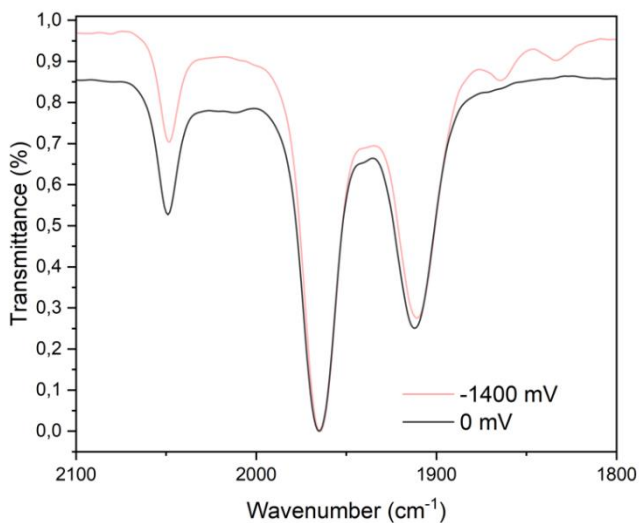


**Figure S13.** IR-SEC reduction of **4** in dry  $\text{CH}_3\text{CN}$  (0.1 M  $[\text{N}(\text{nBu})_4][\text{PF}_6]$ ). The solid lines represent the IR spectra of complex **4** (black) and applying a potential of -1400 mV (red).

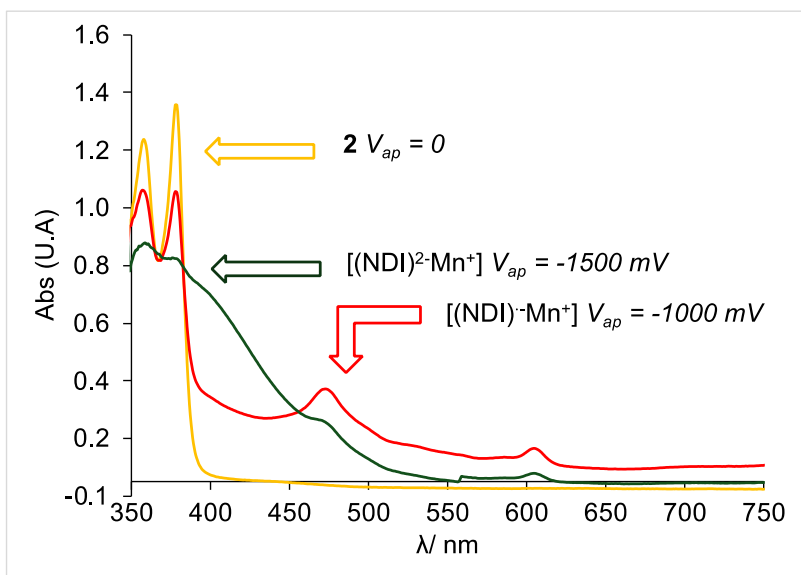


**Figure S14.** UV-Vis-SEC monitoring reduction of **2** in dry  $CH_3CN$  (0.1 M  $[N(nBu)_4][PF_6]$ ). The solid lines represent the UV-Vis spectra of complex **2** (yellow), one-electron reduced species  $[(NDI^{\bullet})Mn^+]$  (red) and two-electron reduced species  $[(NDI^{2-})Mn^+]$  (green).

## 4. Study of the Cl<sup>-</sup>/NDI interaction

### 4.1. Study of the Cl<sup>-</sup>/NDI interaction by IR

The IR spectra of complex **2** were recorded in acetonitrile in the absence and in the presence of different amounts of TBACl (2 and 7 equivalents).

As can be seen in the following figures, the addition of TBACl to a solution of **2** produced changes in the CO frequencies (Figure S15, Table S3) while no changes were observed when adding TBACl to a solution of **4** (Figure S16).

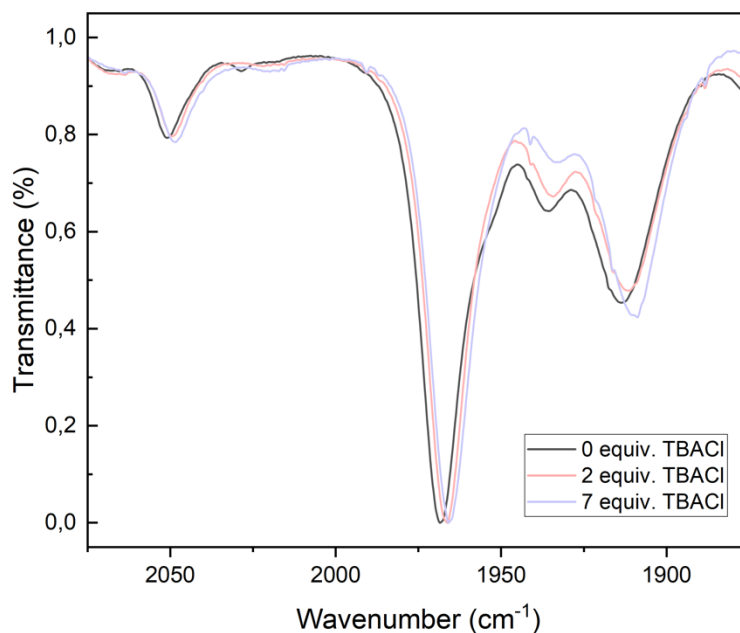


**Figure S15.** IR spectroscopic changes in the spectrum of **2** observed upon the addition of different amounts of chloride [0 equivalents of TBACl (black), 2 equivalents of TBACl (red) and 7 equivalents of TBACl (blue)].

**Table S3.** CO stretching frequencies before and after the addition of TBACl

TBACl added	$\nu_1(\text{CO}) \text{ cm}^{-1}$	$\nu_2(\text{CO}) \text{ cm}^{-1}$	$\nu_3(\text{CO}) \text{ cm}^{-1}$
0 equiv.	2051	1968	1914
2 equiv.	2049	1966	1911
7 equiv.	2048	1963	1909

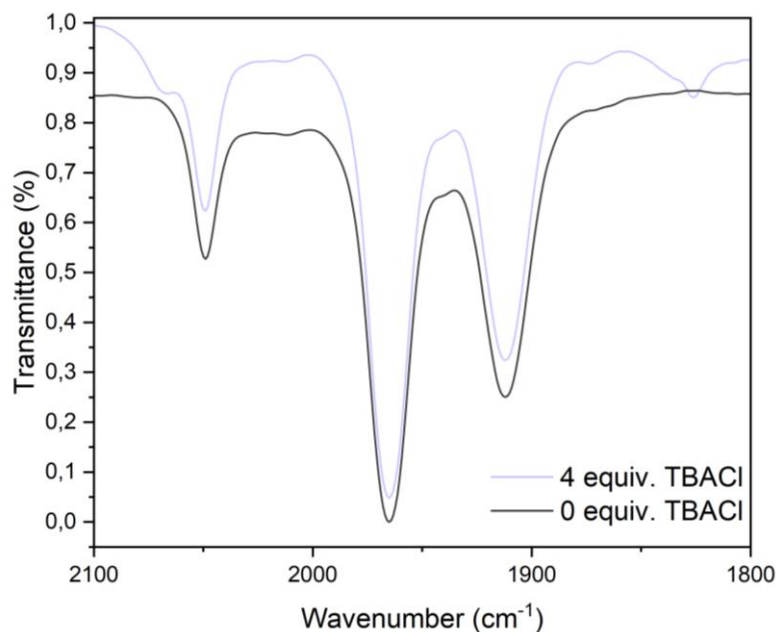


**Figure S16.** IR spectra of **4** before (black) and after the addition of 4 equivalents of TBACl (blue).

#### 4.2. Study of the Cl<sup>-</sup>/NDI interaction by UV-Vis

The UV-Vis spectra of complex **2** was recorded in dry acetonitrile in the absence and in the presence of TBACl (5 equivalents).

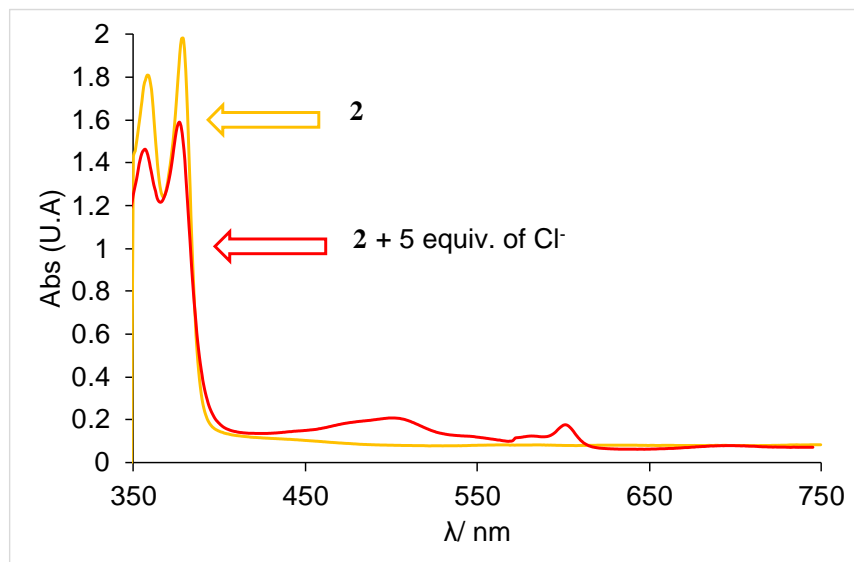


**Figure S17.** UV-vis spectroscopic changes in the spectrum of **2** observed upon the addition of 5 equivalents of TBACl (red).

### 4.3. Study of the Cl<sup>-</sup>/NDI interaction by <sup>1</sup>H NMR

<sup>1</sup>H NMR experiments were performed to determine the effect of the addition of chloride (TBACl) on the resonances of the starting complex **2**. An NMR tube was charged with 0.5 mL of a CD<sub>3</sub>CN solution of complex **2** (8.0 mM). The addition of increasing volumes of a solution of TBACl in CD<sub>3</sub>CN, resulted in a progressive disappearance of the resonances due to the protons of the NDI-NHC ligand, thus indicating the formation of a paramagnetic species.

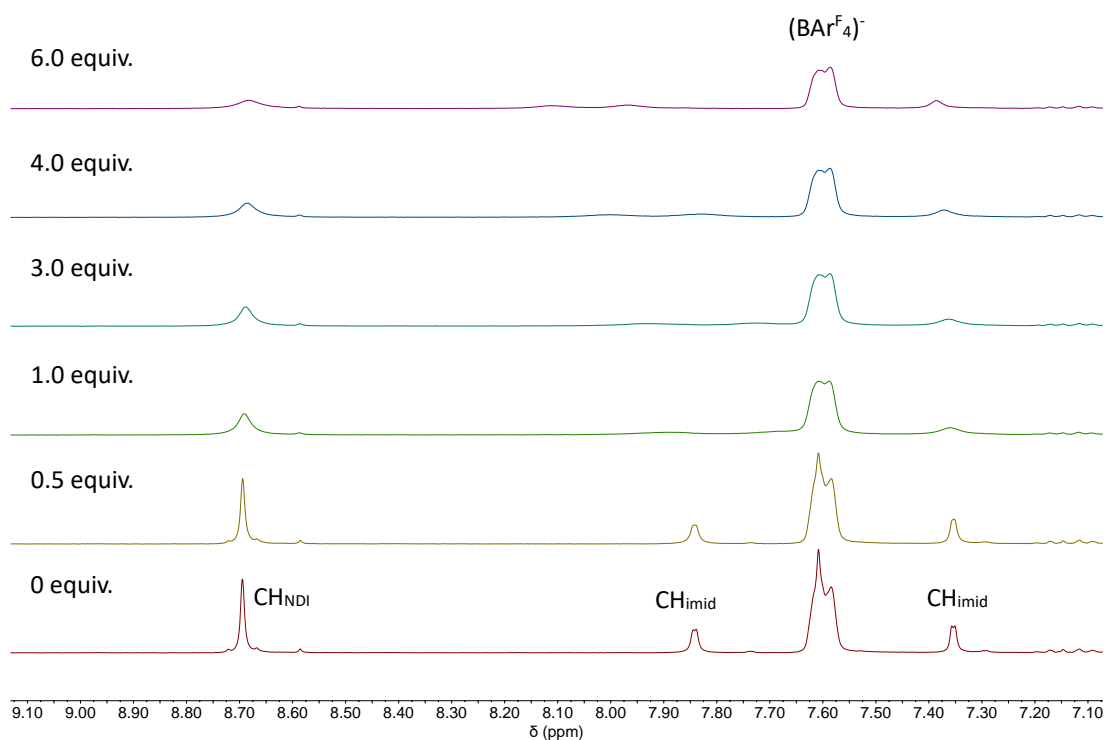
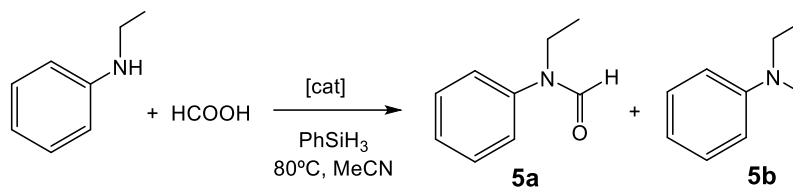


**Figure S18.** Selected region of the <sup>1</sup>H NMR spectra (300 MHz, CD<sub>3</sub>CN, 298 K) of **2** upon the addition of increasing amounts of TBACl.



## 5. Catalytic studies

### 5.1. Formylation/methylation of *N*-ethylaniline using formic acid



**Scheme S2.** Formylation/methylation of *N*-ethylaniline

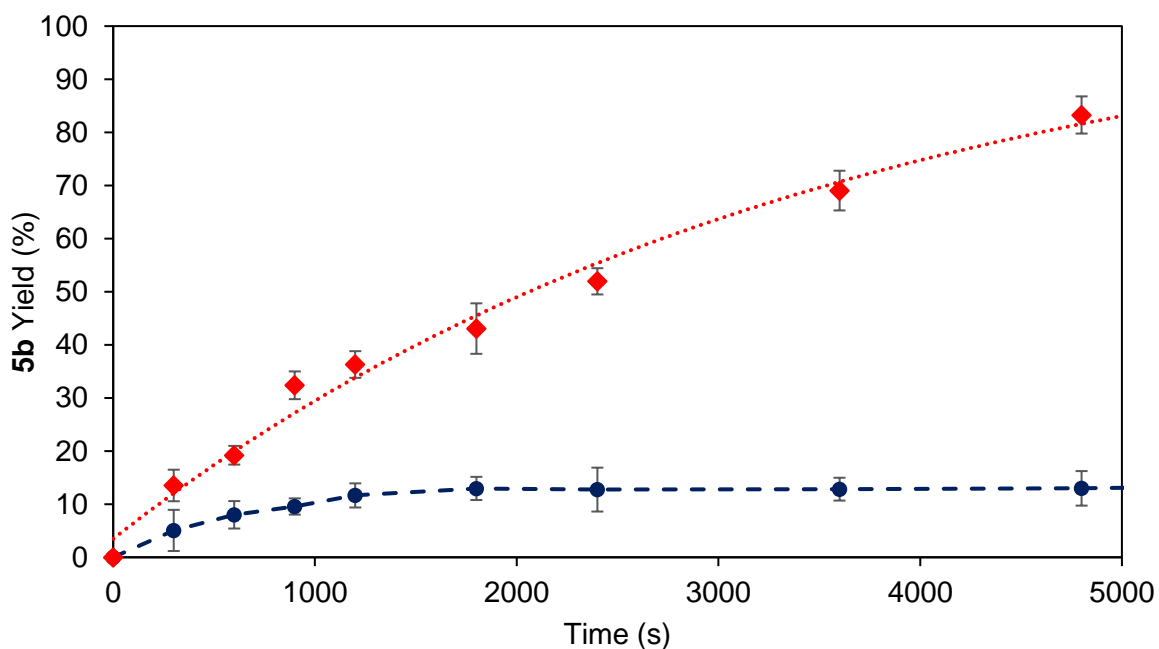
General procedure. All the catalytic experiments and manipulations were conducted under air atmosphere unless otherwise indicated. In a thick-walled glass tube fitted with a Teflon cap, the catalyst (5.0 mol% of complex **2** or **4**) was added to a 0.081 M solution of *N*-ethylaniline (0.081 mmol), phenylsilane (0.486 mmol), formic acid (0.243 mmol) and 1,3,5-trimethoxybenzene (0.0405 mmol) in CH<sub>3</sub>CN (1 mL). The reaction mixture was heated at 80 °C and it was analyzed by <sup>1</sup>H NMR spectroscopy taking an aliquot (20 μL) after 3 hours of reaction. Products were identified according to previously reported spectroscopic data.

Effect of the presence of a chloride source. These experiments were carried out using complex **2** or **4** in the presence of TBACl (20 mol%, 4 equiv.). Figure S19 shows the time-dependent profile of the reaction using complex **2** in the absence (blue) and in the presence of 4 equiv. TBACl (red).

**Table S4.** Formylation/methylation of *N*-ethylaniline using formic acid<sup>[a]</sup>

Entry	Cat. (catalyst loading)	Additive	Conversion (%)	Formylated product (%)	Methylated product (%)
1	<b>2</b> (5 mol%)	none	58	45	13
2	<b>2</b> (5 mol%)	TBACl	100	6	94
3	<b>2</b> (2.5 mol%)	TBACl	92	17	75
4	<b>2</b> (1 mol%)	TBACl	79	37	42
5	<b>4</b> (5 mol%)	none	59	49	10
6	<b>4</b> (5 mol%)	TBACl	88	80	8
7	none	TBACl	88	84	4

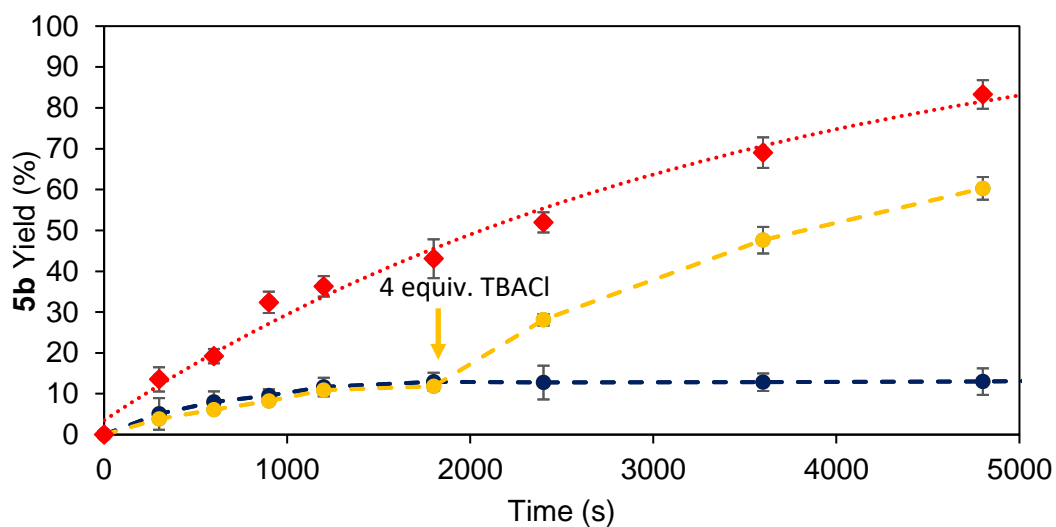
<sup>[a]</sup>The reactions were carried out using complexes **2** and **4** at different catalyst loadings and in the presence of 20 mol% of TBACl where stated, heating at 80 °C for 3h.



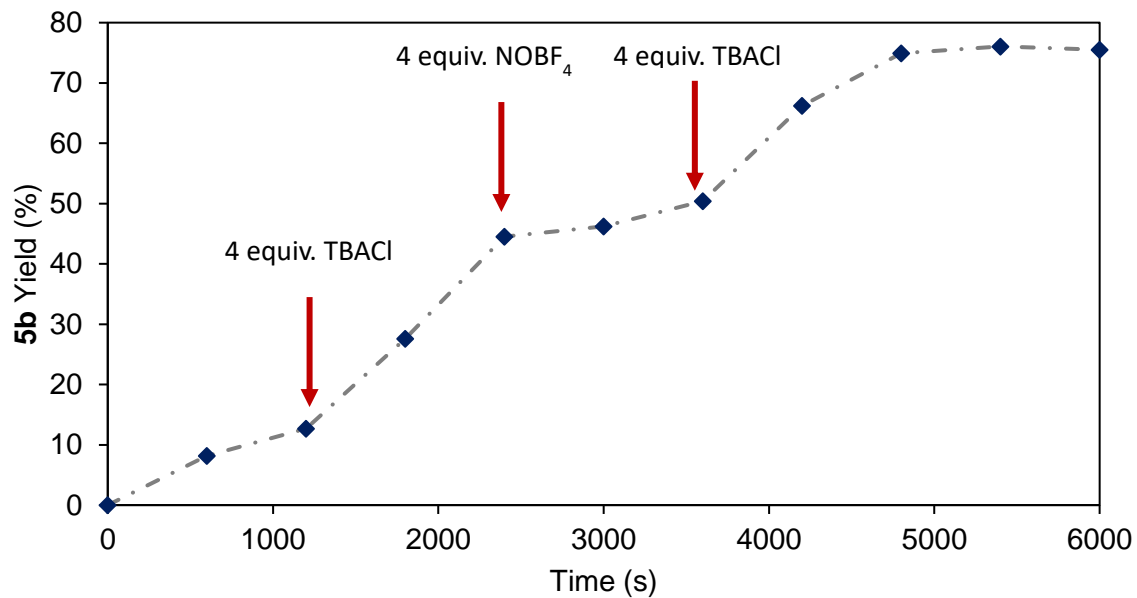
**Figure S19.** Time-dependent reaction profiles for the methylation of *N*-ethylaniline with formic acid and 6 equivalents of PhSiH<sub>3</sub>, using complex **2** in the absence (blue) and in the presence of 4 equiv. TBACl (red).

## 5.2. Redox switching experiments

This experiment was carried out as described above (section 5.1). Figures S20 and S21 shows the time-dependent profile of the reaction initiated with **2** and then subsequently activated and deactivated by addition of TBACl (4 equivalents with respect to catalyst) and NOBF<sub>4</sub> (4 equivalents with respect to catalyst), respectively.



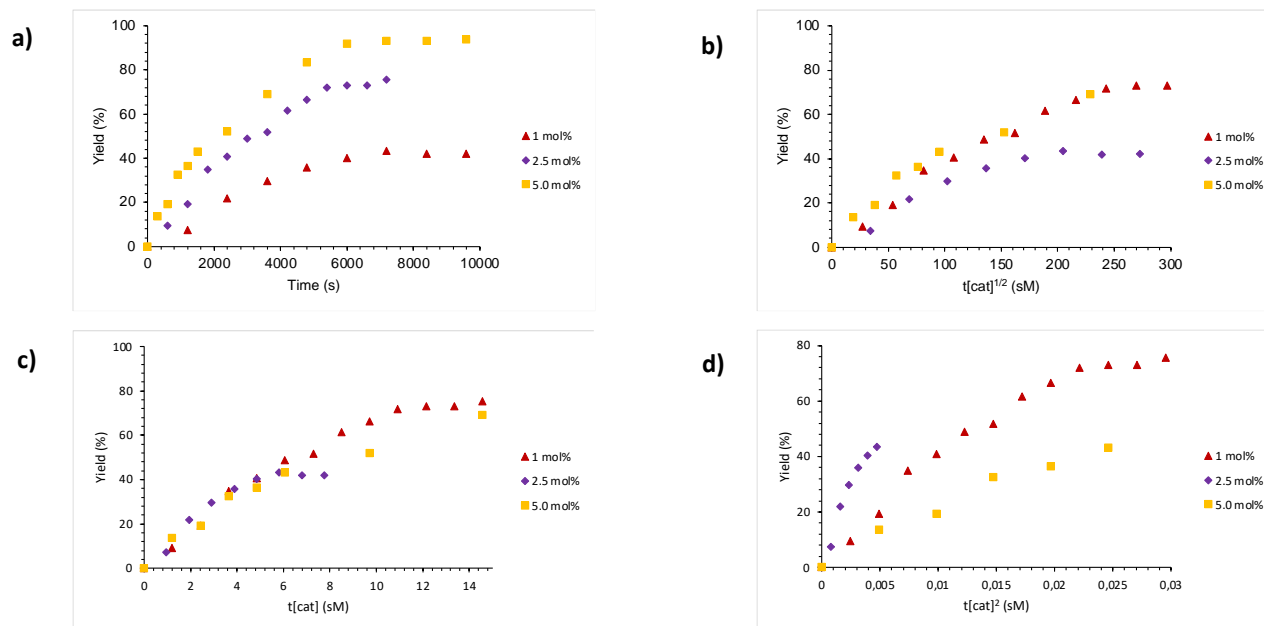
**Figure S20.** Time-dependent reaction profiles for the methylation of *N*-ethylaniline with formic acid and 6 equivalents of PhSiH<sub>3</sub>, using complex **2** in the absence (blue) and in the presence of 4 equiv. TBACl (red). The reaction profile depicted with the yellow dots refers to a reaction that was initiated with **2** alone, and then TBACl was added after 30 minutes of reaction.



**Figure S21.** Time-dependent reaction profiles for the methylation of *N*-ethylaniline with formic acid and 6 equivalents of PhSiH<sub>3</sub>, using complex **2** and with sequential additions of TBACl and NOBF<sub>4</sub>.

### 5.3. Determination of the reaction order with respect to the catalyst

The reaction order with respect to complex **2** was determined by plotting the concentration of the product against a normalized time scale  $t[\text{cat}]^n$  (being  $n$  the order of the catalyst), according to the method developed by Dr. Burés.<sup>4</sup> Visual analysis of the reaction profiles depicted in Figure S19 indicated a first order in **2** (Figure S22c).

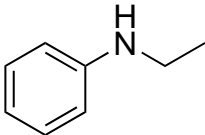
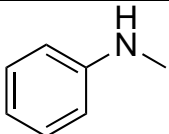
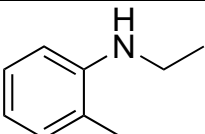
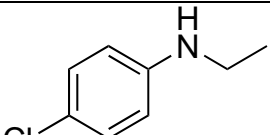
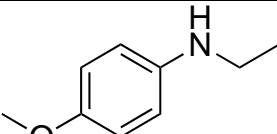


**Figure S22.** (a) Time-dependent reaction profile of the methylation of *N*-ethylaniline. (b) Reaction profile with normalized time scale assuming a catalyst order of 1/2. (c) Reaction profile with normalized time scale assuming a catalyst order of 1. (d) Reaction profile with normalized time scale assuming a catalyst order of 2.

#### 5.4. Study of the scope of the reaction

The reactions were carried out following the general procedure described in section 5.1. In a thick-walled glass tube fitted with a Teflon cap, the catalyst (5.0 mol% of complex **2**) was added to a 0.081 M solution of the corresponding *N*-ethylaniline (0.081 mmol), phenylsilane (0.486 mmol), formic acid (0.243 mmol) and 1,3,5-trimethoxybenzene (0.0405 mmol) in CH<sub>3</sub>CN (1 mL). The reaction mixture was heated at 80 °C and it was analyzed by <sup>1</sup>H NMR spectroscopy taking an aliquot (20 μL) after 3 hours of reaction. Products were identified according to previously reported spectroscopic data. The amount of TBACl used was 20 mol%.

**Table S5.** Formylation/methylation of different amines using **2**

Entry	Amine	Additive	Conversion (%)	Formylated product (%)	Methylated product (%)
1		none	58	45	13
2		TBACl	100	6	94
3		none	95	80	15
4		TBACl	93	20	73
5		none	47	36	11
6		TBACl	85	0	85
7		none	63	58	5
8		TBACl	49	0	49
9		none	76	74	2
10		TBACl	77	0	77

## 5.5. Methylation of *N*-ethylaniline using CO<sub>2</sub>

**General Procedure.** The catalytic experiments were carried out in a Parr Model 4760 General Purpose Pressure Vessel Assembly reactor. In a thick-walled glass tube, complex **2** (5.0 mol %) was added to a 0.081 M solution of *N*-ethylaniline (0.081 mmol), phenylsilane (0.243 mmol), and 1,3,5-trimethoxybenzene (0.0405 mmol) in CH<sub>3</sub>CN (1 mL). The reactor was sealed, and three cycles of pressurization with CO<sub>2</sub> and depressurization were conducted. The reactor was then pressurized with 10 atm of CO<sub>2</sub> and heated at 110 °C. After 12 h, the reactor was allowed to reach room temperature and carefully depressurized. The reaction mixture was analyzed by <sup>1</sup>H NMR spectroscopy taking an aliquot (40 μL) and adding CDCl<sub>3</sub>. Products were identified according to previously reported spectroscopic data.

**Table S6.** Formylation/methylation of *N*-ethylaniline using 10 atm CO<sub>2</sub><sup>[a]</sup>

Entry	Cat. (catalyst loading)	Conversion (%)	Formylated product (5a) (%)	Methylated product (5b) (%)
1	<b>2</b> (5 mol%)	85	77	8
2	<b>2</b> (5 mol%)+ TBACl (20 mol%)	100	9	81
3	TBACl (20 mol%)	70	59	11

## 6. References

- (1) Martínez-Vivas, S.; Gusev, D. G.; Poyatos, M.; Peris, E., Tuning the Catalytic Activity of a Pincer Complex of Rhodium(I) by Supramolecular and Redox Stimuli. *Angew. Chem., Int. Ed.* **2023**, e202313899.
- (2) Peris, E.; Loch, J. A.; Mata, J.; Crabtree, R. H., A Pd complex of a tridentate pincer CNC bis-carbene ligand as a robust homogenous Heck catalyst. *Chem. Commun.* **2001**, 201-202.
- (3) Krejcik, M.; Danek, M.; Hartl, F., Simple construction of an infrared optically transparent thin-layer electrochemical cell applications to the redox reactions of ferrocene,  $\text{Mn}_2(\text{CO})_{10}$  and  $\text{Mn}(\text{CO})_3(3,5\text{-di-}t\text{-butyl-catecholate})$ . *J. Electroanal. Chem.* **1991**, 317, 179-187.
- (4) (a) Bures, J., A Simple Graphical Method to Determine the Order in Catalyst. *Angew. Chem., Int. Ed.* **2016**, 55, 2028-2031; (b) Bures, J., Variable Time Normalization Analysis: General Graphical Elucidation of Reaction Orders from Concentration Profiles. *Angew. Chem., Int. Ed.* **2016**, 55, 16084-16087.